

Design of a Robust Controller for a Tethered Segway on Dome-Shaped Structures

Mohammad H. Salehpour¹ Hamid D. Taghirad² and Hadi Moradi³

^{1,2}Advanced Robotics and Automated Systems, Faculty of Electrical Engineering, K.N. Toosi University of Technology

³Advance Robotics and Intelligent Systems Lab, School of Electrical Engineering, University of Tehran, Tehran, Iran

³Intelligent Systems Research Institute, SKKU, South Korea.

mail: ¹m.h.salehpour@ut.ac.ir, ²taghirad@kntu.ac.ir, ³moradih@ut.ac.ir

Abstract— Tethered Segway is a robotic platform inspired by human climbers. It is a two-wheeled mobile platform tethered to the top of a structure in order to climb steep surfaces with varying slopes, such as domes. The unstructured environment may cause uncertainties in the dynamic behavior of the robot while operating on different parts of the dome. In this paper analysis and synthesis of a robust controller for a tethered Segway is presented in order to provide desired performance in the presence of uncertainties. To design the robust controller, structured and unstructured uncertainties of the model are encapsulated into a structured singular perturbation. A linear robust controller is designed such that the robust stability of the closed loop system is preserved in the presence of modeling uncertainties. Finally, the effectiveness of the proposed controller is verified through simulation by comparing its closed loop transient response and sufficiently suitable steady-state performance to that of a previously proposed LQR controller for the robot.

Keyword—Dome, Segway, Climbing Robot, Robust Control

I. INTRODUCTION

Research on climbing robots has become popular in the field of robotics and mechatronics due to their wide range of applications. One of these applications is the climbing dome-shaped structures for cleaning, inspection, and maintenance purposes. Traditional methods in dome cleaning, inspection, and maintenance performed by human workers have many disadvantages such as danger to the workers and limited operation time [1].

Because of dangerous condition working on steep surfaces and also high demand for autonomous systems in different operations, designing robots to work in these situations has become an interesting research field from both theoretical and practical points of view. Different robots have been developed to climb walls and steep surfaces that uses magnetic systems [2], systems with adhesive materials [3, 4], and suction and vortex [5].

Difficulties and dangers involved in human-based approaches motivate researchers to initiate University of Tehran Dome Robot (UTDR) project. The first system built was a multi-robot platform that could stably cover all parts of a dome [6]. In spite of the novel design of this multi-robot system, its complexity was an issue (Figure 1(a)). Furthermore, the top of domes is the most important area to be inspected and maintained. Thus, a robot that can safely

cover the top part of domes would be enough to handle the majority of tasks needed in dome inspection, cleaning, and maintenance. Consequently, to handle these issues, a single tethered robot, inspired from human dome climbers, was implemented, and successfully tested for dome inspection [1]. This single robot platform may stably cover all parts of a dome with positive slope, as the top existing in a real dome. This robot consists of a simple Segway with differential drive locomotion and a tether mechanism to control the length of the tether while operating on the dome (Figure 1(b)). It is obvious that based on the physics of Segways it cannot stably move on steep surfaces such as domes, due to lack of friction force. Thus, in the design, we added a tether mechanism to stabilize the robot on such surfaces.

It should be mentioned that since Segways are very simple and novel means of transportation and due to their wide range of application in different fields such as robotics, the control of these two-wheeled mobile robots has been the center of interest within the last 15 years. Different controllers have been presented to improve the performance of these mechanisms. [7], [8]. However, to the best of our knowledge, there is no study to analyze and design the controller for a tethered Segway except in [9]. In this paper, the mathematical modeling of a tethered Segway and a simple controller design based on LQR theory and gain scheduling is presented. Simulations show that the designed linear controller, applied to this non-linear system, can provide suitable performance for predetermined slopes.

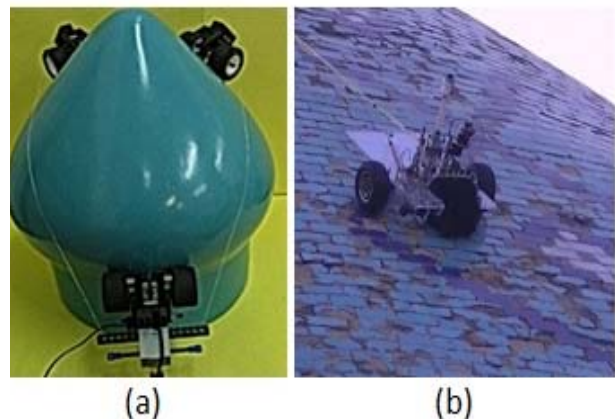


Figure 1. (a) The multi-robot platform to climb the dome-shaped structures. (b) Dome Tethered Robot climbing the dome

*This project is partially supported by Hosseinie Ershad Foundation

However, a dome's slope varies while moving along the dome which causes the parameters to vary during the movement and the designed controller may not be robust to such variations. To overcome this issue linear adaptive or gain scheduling controllers may be implemented in real-time. However, this may cause additional problems due to their high rate of slope change, and instability dangers.

In this paper we present a single controller, using robust control synthesis [10] [11], which is stable and performs well for all possible operation conditions of the system.

II. MODELING AND THE ANALYSIS

A. System Model

In this section first, we briefly restate the UTDTR system specifications so as we can present the rest of this work. Simply consider the UTDTR system as a tethered Segway on a dome (Figure 3). The UTDTR system specifications and detailed approach to finding the mathematical equations of the system using Euler-Lagrange formulation is discussed in [9]. It is shown that the UTDTR system may be modeled with a nonlinear time-invariant system with following dynamic equations:

$$\ddot{\theta} = f_1(\dot{\theta}, \dot{\phi}, \psi, \dot{\psi}, \theta_d, k, v_r, v_l) \quad (1)$$

$$\ddot{\phi} = f_2(\dot{\phi}, \psi, \dot{\psi}, v_r, v_l) \quad (2)$$

$$\ddot{\psi} = f_3(\dot{\theta}, \dot{\phi}, \psi, \dot{\psi}, \theta_d, k, v_r, v_l, v_t) \quad (3)$$

In these formulation, θ, ϕ, ψ represent system's motion variables which denote the average angle of the left and right wheel, body yaw angle, and body pitch angle, respectively. Furthermore, v_r, v_l, v_t are input voltage commands to the DC-motors. θ_d and k are the slope of the dome and the rope's tension factor relating to the environment condition. Therefore, the nonlinear state space formulation for the system may be presented as follows:

$$x = [\theta, \dot{\theta}, \phi, \dot{\phi}, \psi, \dot{\psi}]^T, u = [v_r, v_l, v_t]^T \quad (4)$$

$$\dot{x} = f(x, u, \theta_d, k) \quad (5)$$

$$y = [\theta, \phi, \psi]^T \quad (6)$$

whose details may be found at the following links:

[SOD NonlinearModel](#)
[SOD NominalParameters](#)

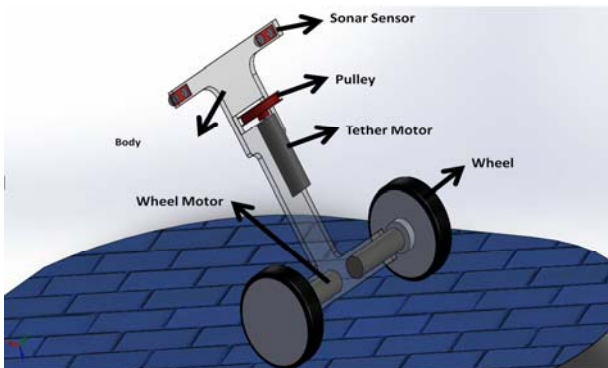


Figure 3. Tethered Segway schematics with a motor controlling the length of the tethered attached to the top of a steep surface.

B. Stability Analysis and Nominal System

In the above formulations θ_d and k are environment parameters depending on the position of the robot on the dome surface. The slope of the dome varies in a range of 15 to 75 degrees in most real structures. Let us present a simple analysis on how the parameter k varies as the robot moves on the dome surface. Parameter k equals to $\cos\theta_t$ where θ_t is the angle of rope. It is shown in Figure 2 that this angle varies between -15 to 15 degrees in complete coverage of robot on surfaces with a positive slope. Therefore, the environment variable k lies in a range of $[0.9, 1]$, and nominal values for θ_d and k are as follows:

$$\theta_{dn} = 45^\circ, k_n = 0.95 \quad (7)$$

Nominal values for other parameters of the system are prescribed in [9]. Using these nominal parameters, the open-loop response of the system is illustrated in Figure 4, which is obviously unstable. Since the procedure to design a robust controller with desired performance for a nonminimum-phase and unstable system may encounter serious problems. first let us stabilize the system using a state feedback controller. Meanwhile, in the first step we linearize the system using the nominal values around equilibrium point at the origin. Then by using pole-placement we design the proper gain, K_s in the state feedback law. Applying this gain to the nonlinear system would cause a stable closed-loop nonlinear system with the following dynamic equations:

$$u = r - K_s x \quad (8)$$

$$\dot{x} = f(x, r - K_s x, \theta_d, k) = f_s(x, r, \theta_d, k) \quad (9)$$

$$y = [\theta, \phi, \psi]^T \quad (10)$$

Using these nominal parameters, the new closed-loop system is asymptotically stable about the equilibrium point. Hence, consider the system as the plant and design the robust linear controller for this system.

III. ROBUST CONTROL DESIGN

Now that the UTDTR system's specifications and its model have been presented, and furthermore, an inner loop controller is designed to stabilize the system, one may proceed to design a robust controller for such system. Simulation of the stabilized system shows that the performance of the system with this simple controller is far

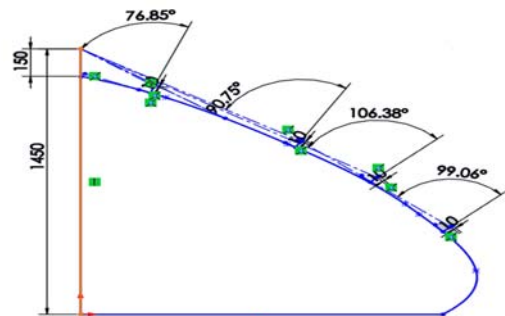


Figure 2. Analysis on how θ_t varies as the robot moves along a sample dome. This analyze is done on Imam Reza's dome, Mashhad, Iran.

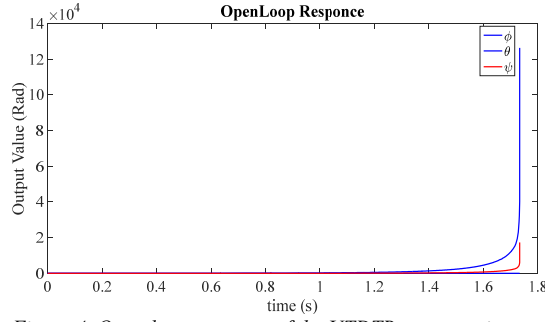


Figure 4. Open-loop response of the UTDTR system to input vector $u = [-6, -6, -6]^T$

from the desired behavior in terms of robust stability, suitable tracking with fast response, and disturbance attenuation in the presence of limited control effort. In order to obtain the desired performance, the problem is well suited to reformulate into an H_∞ or μ synthesis optimization. In this section, the problem is reformulated such that these methodologies can be applied.

A. Uncertainty Modeling of the UTDTR System

In order to apply H_∞ and μ synthesis to this problem, we have to encapsulate all uncertainties of the system. Since these methods are being applied to the linearized model, beside the prescribed parametric uncertainties, there is an unstructured uncertainty caused by linearization. Therefore, one may encapsulate the whole uncertainties with input multiplicative uncertainties. In order to perform that, first consider $W_p \Delta_p$, for parametric uncertainties, and then $W_l \Delta_l$, for linearization uncertainties as depicted in Figure 5. It seems better to combine these uncertainties and form a global uncertainty and represent it as a multiplicative uncertainty in the input as below:

$$G = G_0(I + W_l \Delta_l)(I + W_p \Delta_p) \quad (11)$$

$$G = G_0(I + W_l \Delta_l + W_p \Delta_p + W_l W_p \Delta_l \Delta_p) \quad (12)$$

Where G and G_0 are, respectively, the UTDTR true and nominal linearized models with nominal parameters representing the system. Assume Δ such that:

$$\Delta > \max\{\Delta_l, \Delta_p\} \quad (13)$$

Then, one may conclude that:

$$(W_l + W_p + W_l W_p) \Delta > W_l \Delta_l + W_p \Delta_p + W_l W_p \Delta_l \Delta_p \quad (14)$$

Therefore, the total uncertainty may be represented as:

$$G = G_0(I + (W_l + W_p + W_l W_p) \Delta) \quad (15)$$

$$W = (W_l + W_p + W_l W_p) \quad (16)$$

Two stage uncertainty generation has been done instead of a one-stage method. This is due to the fact that the range of the variables that construct uncertainty and also desired variation about the linearization point is a wide range. Therefore, uncertainty derivation in a single stage may need a high amount of calculation, while the prescribed procedure helped us to construct the uncertainty easier and faster. Now let us encapsulate the individual uncertainty weighting functions

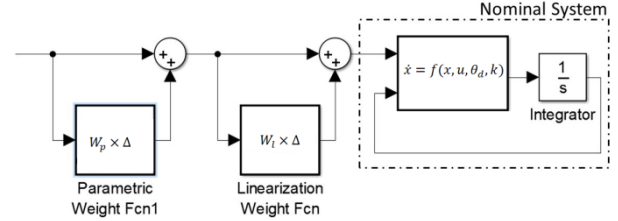


Figure 5. Uncertainties of the UTDTR system modeled with input multiplicative uncertainties.

W_l, W_p which is used to construct the uncertainty weight function using (16).

a. Linearization Uncertainty

The nonlinear model of UTDTR may be represented by a linear model and the multiplicative uncertainty in the input, using spectral identification scheme. In this representation, the nominal model replicated the dynamic behavior of the system, only at nominal conditions, and all nonlinear interactions, unmodeled dynamics, and disturbances are encapsulated with an unstructured uncertainty representation. Let us replace all the parameters in (9) to their nominal values and name the resulting nonlinear model, as P .

$$P = G_0(I + W_l \Delta_l) \quad (17)$$

In this equation, W_l is a stable transfer function indicating the upper bound of the uncertainty profile and Δ_l indicates the admissible uncertainty block, which is a stable but unknown transfer function with $\|\Delta_l\|_\infty < 1$. To calculate the W_l weighting function we have:

$$\Delta_l(j\omega)W_l(j\omega) = \frac{P(j\omega)}{G_0(j\omega)} - I \quad (18)$$

In which $\|\Delta_l\|_\infty < 1$. Hence,

$$\|W_l(j\omega)\| \geq \left\| \frac{P(j\omega)}{G_0(j\omega)} - I \right\|, \forall \omega \quad (19)$$

In order to analyze frequency response of the plant, we linearize it at different operation points. Considering the fact that all nonlinear terms in P are only functions of ψ and having in mind that one of the objectives in this problem are to regulate the ψ angle to 0° , we can analyze the plant about different values of the system variable ψ in the small range about the origin like $\psi \in [-\pi/6, \pi/6]$. Figure 6 shows the singular value plot for right-hand-side of (18). As UTDTR

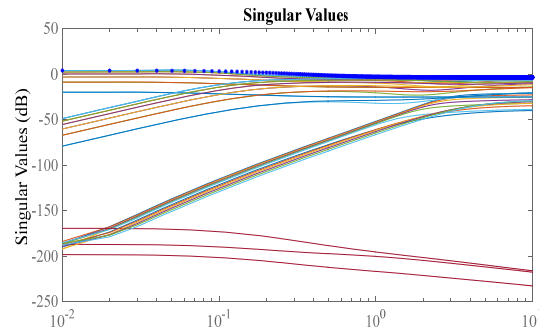


Figure 6. Singular values for $G_0^{-1}P - I$ for different systems for $\psi \in [-\frac{\pi}{6}, \frac{\pi}{6}]$

system is a MIMO (3input-3output) system, therefore, the maximum singular value of a system represents the norm of admissible uncertainty block. The least upper bound of the uncertainty profiles is determined as weighting function W_l , which is plotted in with stars in Figure 6 and its transfer function is as bellow:

$$W_l(s) = \frac{0.6546s + 0.5891}{s + 0.3835} \quad (20)$$

b. Parametric Uncertainty

Considering the nominal system, G_0 and all perturbed systems caused by parametric uncertainties in P , in this section, we are going to find weighting function of the multiplicative uncertainty modeling systems behavior in presence of parameter deviations. Consider:

$$G_m = G_0(I + W_p \Delta_p) \quad (21)$$

where G_m is a true model of UTDTR system with parameters deviation from their nominal values. Analysis prescribed in (18) and (19) would be held for G_m instead of P to find the parametric weight function, W_p . Uncertain parameters in the UTDTR and their nominal values are introduced in section II.B. What is plotted in Figure 7 is the maximum singular value of $G_0^{-1}G_m - I$ for different values of uncertain parameters. This figure shows that the difference between all the perturbed systems and the nominal system, may be fitted with the least upper bound W_p in which is plotted in stars, and its transfer function is as bellow:

$$W_p(s) = \frac{0.7161s + 0.358}{s + 0.6294} \quad (22)$$

Using equation (16) the overall weight function may be derived as bellow:

$$W(s) = \frac{1.839(s + 0.383)(s^2 + 1.245s + 0.39)}{(s + 0.629)(s + 0.383)} \quad (23)$$

B. Controller Design

In order to design robust controllers to provide desired behavior, prescribed in III we have to determine the control effort and performance weight functions W_u and W_s , respectively. DC-motors in the UTDRT system can work with input voltages from -12^V to 12^V . Therefore, the control effort weight function may be selected as a constant function:

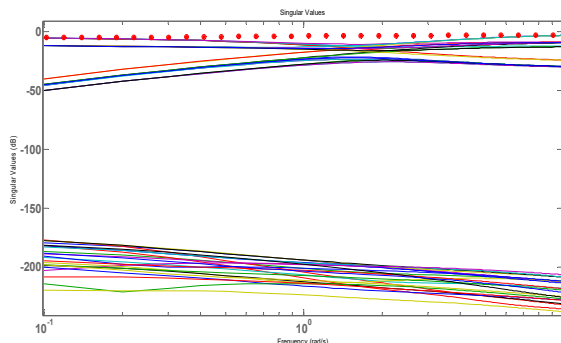


Figure 7. Singular values for $G_0^{-1}G_m - I$ for different systems for $\theta_a \in [15,75]^\circ$ and $k_n \in [0.9,1]$

$$W_u(s) = \frac{I_{3 \times 3}}{12} \quad (24)$$

In order to specify the desired performance weighting function, let us determine the desired closed-loop transfer function T for UTDTR. Preferred performance for UTDTR is tracking set-points with low steady state error, minimum overshoot and settling time. In the first step let us consider the desired closed-loop systems response to strictly satisfy all of the above conditions, for steady state error set to zero and $T_s < 5s$ and $\%OS < 1\%$. This may be represented with a simple second order system with the following transfer function:

$$T_{id} = \frac{1}{s^2 + 1.7s + 1} \quad (25)$$

So using (25) we have:

$$S_{id}(s) = \frac{s^2 + 1.7s}{s^2 + 1.7s + 1} \quad (26)$$

$$W_s(s) = \frac{s^2 + 1.7s + 1}{s^2 + 1.7s + 0.01} I_{3 \times 3} \quad (27)$$

Objectives of the problem described above can be simultaneously optimized by the solution of a mixed sensitivity problem. Which is providing the controller such that the inequality bellow is held:

$$\begin{bmatrix} W_s S \\ W_u u \\ WT \end{bmatrix} < 1 \quad (28)$$

also to design the μ controller we shape the control loop as in Figure 8, and the next step is to solve the mixed sensitivity problem and the μ -synthesis problem to design individual controllers with aid of robust control toolbox in MATLAB (`hinfscyn` and `dkscyn` commands) which may result in two high-order controllers. Some specifications about the resulting controllers are represented in TABLE II. TABLE IAs we can see, the achieved gamma with these weighting functions is more than one in both H_∞ and μ -synthesis methods. This means that there is no guarantee that the closed-loop system is stable in all the conditions with these controllers. Thus we need to relax the constraints in order to design a robust controller satisfying the following robust stability condition:

$$\|WT\|_\infty < 1 \quad (29)$$

where W is the uncertainty weight function and T is the closed-loop system. which is equivalent to the weighted complementary sensitivity function. (small gain theorem [12]).

In the next step let us reduce the uncertainty profile by assuming that our objectives are to design a suitable controller for values of the system variable ψ in a smaller range of $\psi \in [-\pi/12, \pi/12]^{rad}$. By recalculation for the linearization multiplicative uncertainty weighting function as before, the singular value plot for right-hand-side of (18) when $\psi \in$

TABLE I. SPECIFICATIONS FOR H_∞ AND μ -SYNTHESIS CONTROLLERS IN FIRST STEP

Method	Gamma achieved	Controller Order
Mixed sensitivity(H_∞)	4.2848	18
μ - synthesis	3.159	24

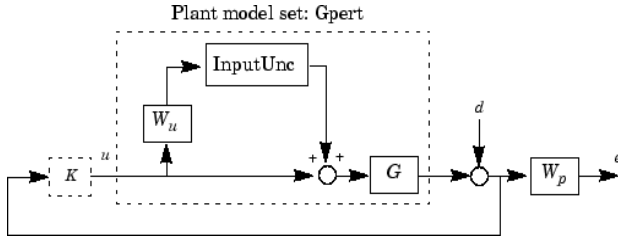


Figure 8. Closed-loop structure for Robust control design for UTDR robotic system

$[-\pi/12, \pi/12]^{rad}$ is plotted in Figure 9. The least upper bound of the uncertainties W_l , in this case, is plotted in this figure with stars and its transfer function is as below:

$$W_l(s) = \frac{0.338 + 0.06338s}{s + 0.3} \quad (30)$$

By assuming the W_p as before, given in (22) the total multiplicative weight function may be derived as:

$$W(s) = \frac{1.2961(s + 0.5409)(s + 0.2425)}{(s + 0.6294)(s + 0.3)} \quad (31)$$

We may relax the performance constraints such that we may achieve the stability condition prescribed in (29). For instance, we may consider the closed-loop system to track the set-point with 10% steady state error. Also, overshoot percentage less than 15% is admissible and settling time less than 10 seconds can satisfy our objectives. By these relaxations the desired closed-loop system is considered as a second order system with the following transfer function:

$$T_{id} = \frac{0.9}{s^2 + 1.4s + 1} \quad (32)$$

So using (32) we have:

$$S_{id}(s) = \frac{s^2 + 1.4s + 0.1}{s^2 + 1.7s + 1} \quad (33)$$

$$W_s(s) = \frac{s^2 + 1.4s + 1}{s^2 + 1.4s + 0.1} I_{3 \times 3} \quad (34)$$

Using robust control toolbox in MATLAB H_∞ and the μ controller is redesigned. Gamma achieved in the mixed sensitivity and μ -synthesis problem (about 1.4 for H_∞ controller and 1.45 for μ controller), are sufficiently close to one. The designed controllers are high-order MIMO systems (18th order for H_∞ controller and 24th order system for μ controller), so using order reduction methods we reduce these controllers to 10th order systems. Applying the reduced

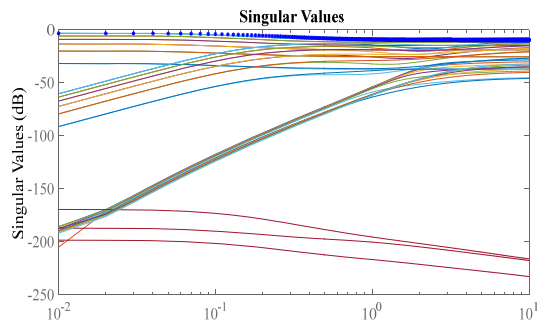


Figure 9. Singular values for $G_0^{-1}P - I$ for different systems for $\psi \in [-\frac{\pi}{12}, \frac{\pi}{12}]$

TABLE II. STEP RESPONSE BEHAVIOR FOR 1000 CLOSED-LOOP SYSTEMS APPLYING C_{H_∞} AND C_μ

Controller	Maximum %OS	Satisfying %OS condition	Maximum T_s (s)	Satisfying T_s condition
C_{H_∞}	17.58 %	99.6%	24.54	96.9%
C_μ	27.86%	99.1%	36.47	98.5%

order controllers to the real system with the structure represented in Figure 1, we would have two different closed-loop systems. Let's name the controller designed through the H_∞ method C_{H_∞} and the controller designed with μ -synthesis as C_μ . You can get the designed controllers here using the following link: [SOD RobustControllers](#)

IV. PERFORMANCE ANALYSIS OF C_{H_∞} AND C_μ AND COMPARISON WITH LQR CONTROLLER

Now let's analyze the closed-loop system's behavior using each controller. We may apply these controllers to 1000 different perturbed systems with different parametric and unstructured perturbations. In all of these sample systems, the closed-loop system is stable. As UTDR is a MIMO (3input-3output) system we consider maximum overshoot (OS%), undershoot(US%) and settling time(T_s) of all 9 channels of the system as the %OS, US%, and T_s . TABLE II shows the results for a mean of these two closed-loop systems for all the perturbed systems. Information given in this table indicates that the system is behaving sufficiently suitable for almost every possible situation for the UTDR robotic system. Note that environment parameters, θ_d and k , causing parametric uncertainty in the system's model change gradually as the robot is moving along the dome. This means that those rare conditions, in which the closed-loop system does not behave as desired cannot last more than a few seconds and the system can behave as desired as it passes these conditions.

Now let's apply these controllers to the nonlinear model of the system and verify their performance. Figure 10 (a) shows the results for the UTDR closed-loop system in an extreme case, in which structured and unstructured uncertainties are at their maximum, controlled by C_{H_∞} and C_μ . System outputs and control effort signals in presence of noise and disturbance are plotted in Figure 10 (b). As it is seen in this figure, the UTDR system can track set-points with desired behavior as prescribed before. Furthermore, the control effort lies in the feasible range of $[-12^v, 12^v]$, during the transient and steady state phase (Figure 10 (b)). These results clarify that by using C_{H_∞} and C_μ in the closed-loop system the steady-state responses are close to each other, while their transient responses are different. It can also be seen that using the C_{H_∞} controller, needs smaller control effort than using the C_μ cothe

TABLE III. COMPARISON BETWEEN UTDR CLOSED-LOOP BEHAVIOR USING C_{H_∞} , C_μ , AND LQR CONTROLLERS

Controller	OS%	US%	T_s (s)	E_{ss}
C_{H_∞}	0.976 %	-	2.31	6.34%
C_μ	1.015%	-	1.78	7.08%
LQR	8.746%	34.297%	8.34	9.32%

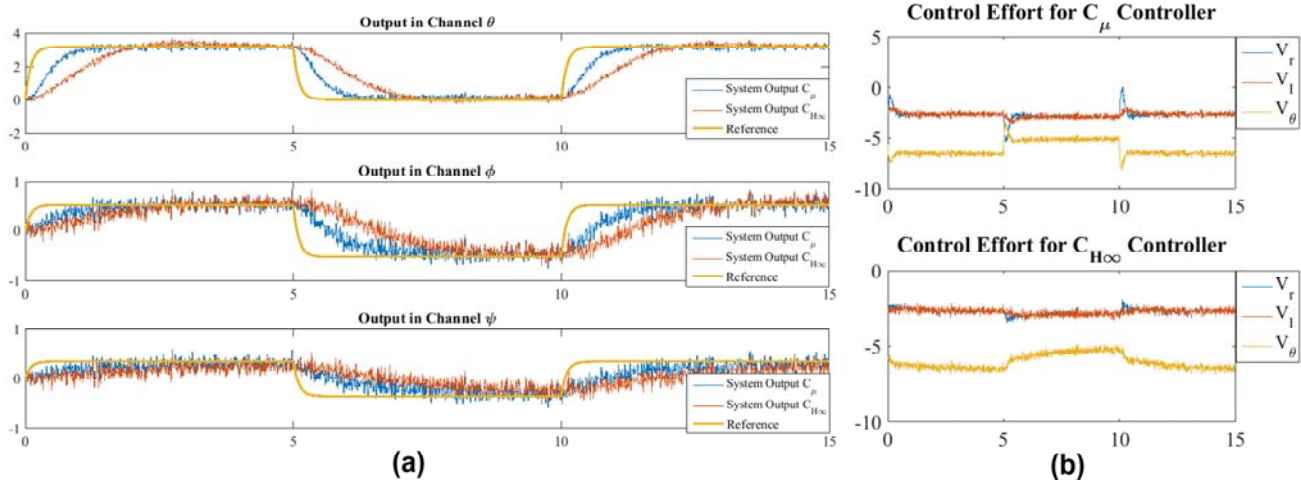


Figure 10. (a) Output for different channels using C_{H_∞} and C_μ in the closed-loop system. (b) Control effort for different inputs, using C_{H_∞} and C_μ in the closed-loop system.

controller in the closed-loop system. Now let's compare the performance of these robust controllers with the performance of the previously proposed LQR controller in [9]. TABLE III contains the information of the closed-loop system with robust controller and the LQR controller in the same condition with the same parameters. Using the robust controller, we can obtain 5 times faster closed-loop system in comparison with the LQR controller. Also, the LQR controller causes undershoot (US%) and high overshoot percentage in comparison to the robust controller because we have used a second order closed-loop behavior in our design procedure the designed controller caused no right-hand side zero in the closed-loop system and there is no undershoot (US%) in the resulting behavior. As it is clear in Figure 10 the μ -controller is much faster than the H_∞ controller and both of the designed controllers can track the step set-points as well. More details about designed controller's behavior have been provided in TABLE III. Note that values reported in this table is the maximum value of different channels for these values.

V. CONCLUSION AND FUTURE WORK

In this paper, we introduced two robust controllers for a tethered Segway, which can be highly applicable in situations in which a normal Segway is not capable of operation. The controllers have been analyzed and their robust stability has been presented. The controllers have been simulated on steep surfaces confirming the analytical results. The result shows that the system can stably move on steep surfaces, ranging from 15 degrees to 75 degrees elevation.

We plan to experimentally implement the proposed controller on the Dome Tethered Robot described in [1] and test the controller in action. Furthermore, a path planning algorithm would be designed to plan the trajectory of the robot from a given point to the desired point on a dome surface.

ACKNOWLEDGMENT

We like to thanks, Dr. F. Farivar for her feedback and help during the research. Also, we may thank A. Nejadfard for his help initiating the project. This project is partially funded and

supported by Hosseinieh Ershad foundation and it is fully funded by the Iranian National Science Foundation

REFERENCES

- [1] M. H. Salehpour, B. Zamanian, and H. Moradi, "The design, implementation, and stability analysis of a human-inspired dome-tethered robot," in *2014 Second RSI International Conference on Robotics and Mechatronics (ICRoM)*, 2014, pp. 648–653.
- [2] M. Tavakoli, C. Viegas, L. Marques, J. Norberto, and A. T. de Almeida, "Magnetic omnidirectional wheels for climbing robots," in *2013 IEEE/RSJ International Conference on Intelligent Robots and Systems*, 2013, pp. 266–271.
- [3] O. Unver, A. Uneri, A. Aydemir, and M. Sitti, "Geckobot: a gecko-inspired climbing robot using elastomer adhesives," in *Proceedings 2006 IEEE International Conference on Robotics and Automation, 2006. ICRA 2006.*, pp. 2329–2335.
- [4] D. Schmidt and K. Berns, "Climbing robots for maintenance and inspections of vertical structures—A survey of design aspects and technologies," *Rob. Auton. Syst.*, vol. 61, no. 12, pp. 1288–1305, Dec. 2013.
- [5] Y. Yoshida and S. Ma, "Design of a wall-climbing robot with passive suction cups," in *2010 IEEE International Conference on Robotics and Biomimetics*, 2010, pp. 1513–1518.
- [6] A. Nejadfard, H. Moradi, and M. N. Ahmadabadi, "A multi-robot system for dome inspection and maintenance: Concept and stability analysis," in *2011 IEEE International Conference on Robotics and Biomimetics*, 2011, pp. 853–858.
- [7] H. G. Nguyen, J. Morrell, K. D. Mullens, A. B. Burmeister, S. Miles, N. Farrington, K. M. Thomas, and D. W. Gage, "Segway robotic mobility platform," in *Optics East*, 2004, pp. 207–220.
- [8] Vijayanand Kurdekar1, "Inverted Pendulum Control: A Brief Overview," *Ijmer*, vol. 3, no. 5, pp. 2924–2927, 2013.
- [9] M. Salehpour, H. Moradi, "The Analysis and Simulation of a Tethered Segway," in *2015 Second RSI/ISM International Conference on Robotics and Mechatronics (ICRoM)*, 2015.
- [10] G. Zames, "Feedback and optimal sensitivity: Model reference transformations, multiplicative seminorms, and approximate inverses," *IEEE Trans. Automat. Contr.*, vol. 26, no. 2, pp. 301–320, Apr. 1981.
- [11] K. Zhou and J. C. Doyle, "Essentials of robust control," *Automatica*, vol. 38, no. 5, pp. 910–912, 2002.
- [12] J. Doyle, B. Francis, A. Tannenbaum, *Feedback Control Theory*, Macmillan 1990